AGU PUBLICATIONS

Geophysical Research Letters

Supporting Information for

High injection rates counteract formation of far-reaching fluid migration pathways at The Geysers geothermal field

Stanisław Lasocki[1], and Beata Orlecka-Sikora[1]

[1]Institute of Geophysics Polish Academy of Sciences

Contents of this file

Introduction

Text S1 presents briefly the transformation to equivalent dimension technique. This transformation was applied to eight parameters that represented seismic events in calculations of the degree of disordering of sources, *ZZ*. *ZZ* was determined by distances between the events seen as points in 8D space of these parameters. *ZZ* could not be evaluated from original values of these parameters because these parameters were not comparable and five of them did not have the Euclidean metric. The transformation to equivalent dimensions is suited for such problems. After transformation any set of parameters becomes comparable and the parameter space metric becomes Euclidean. The text S1 presents the problem, provides the assumptions of the transformation, defines equivalent dimensions, presents their properties and the algorithm of the transformation. The address of the web page from where the MATLAB codes of the transformation can be downloaded is also provided.

Figures S1 to S4 present the locations of hypocenters of the analyzed seismic events in the 3D view and in the three 2D projections. The events marked by blue circles indicate locations of the event from the cluster A, which have been analyzed in this paper. The other events from the initial dataset are marked by black squares. The size of markers is proportional to the magnitude of events. Locations of the open holes of the injection wells Prati9 and Prati29 are also provided.

Figures S5 presents magnitude distribution of all events as well as of the events from particular injection phases.

Figure S6 presents the scatterplots of the degree of disordering of sources, *ZZ* vs. the average injection rate into Prati9 well, *IN*(9), in the injection phases F1 and F2.

Tables S1-S4 compliment Table 2 and present the results of the correlation analysis between the injection rate, *IN*, and the degree of disordering of sources, *ZZ* and the three components of *ZZ* for the *ZZ* and its components delayed with respect to *IN* values from zero to 21 days, step one day. Table S1 contains the results for the injection phase F1, Tables S2 and S3 contain the results for the injection phase F2 and Table S4 contains the results for the injection phase F3. The results in Table S2 relate to the correlations with the injections into the injection well Prati9 and the results in Table S3 relate to the correlations with the summed injections into Prati9 and Prati29 wells.

Text S2 compares the results of correlation analysis between injection rate and three different representations of closeness of hypocenters namely: (1) the average distance between hypocenters in equivalent dimension space, Δ_r – the parameter used in the main text, (2) the correlation dimension of distance between hypocenters, (3) the summarized squared distance between hypocenters in original Cartesian system of coordinates. The comparison has been performed on the data from phase F1.

In Text S3 we present a possible explanation of the obtained in phase F3 anticorrelation between the degree of disordering of sources, *ZZ*, and the injection rate.

Text S1. Summary of the transformation to equivalent dimension technique (Lasocki, 2014)

Parameters of Seismic Events

- Source parameters: *t, lat, lon, depth, M,* $[M_{i,j}]$, E_s, $\Delta\sigma$, r_0 etc.
- Derived from source parameters of two or more events e.g.: interevent time - τ, distance between this and the main shock - *r*, etc.
- Other having unambiguous association with seismic events e.g.
  - Parameters of the environment in which the event occurs: e_1, e_2, e_3
  - Parameters of inducing technological activity for anthropogenic seismicity: l_1, l_2, l_3 ...
  - …………………………………

A seismic event ≡ A point in a parameter space e.g. : **X**= [t, lat, lon, $depth$, M, $[M_{i,j}]$, E_s $\Delta\sigma$, r_0, …, τ, r, …, e_1, e_2, e_3, ..., l_1,l_2, l_3, ..., ...]

Problem: Parameters of seismic events are not comparable and may have non-Euclidean metric.

Equivalent dimensions – Assumptions:

- Let seismic events be represented by the set of parameters X_k, k=1,..,p,. The population of these events is fully characterized by the probabilistic distributions of the parameters $F(X_k)$, k=1,..,p.
- Two intervals of the parameter values, $[x_{k,i},x_{k,j}]$, $[x_{l,s},x_{l,t}]$ are equivalent if $\mathrm{Prob}(X_k \in [x_{k,i},x_{k,j}]) = \mathrm{Prob}(X_l \in [x_{l,s},x_{l,t}])$.
- The parameters X_k, k=1,..,p, are continues random variables.

Equivalent dimension – Definition: The equivalent dimension of X is $U=F(X)$, where $F(X)$ is the cumulative distribution of X

Properties

- Every U is uniformly distributed in [0,1]
- $\{U_{i=1,..p}\}$ has Euclidean metric
- The distance between the two seismic events, i, j , is

$$d(i,j) = \sqrt{\sum_{k=1}^{p} [U_k(i) - U_k(j)]^2}$$

Technique

- The probabilistic models for earthquake parameters, $F(X_k)$, are in general not known.
- If the earthquakes' data are a representative sample of size n, replace $F(X_k)$, k=1,..,p with their data-driven, kernel estimators (Silverman, 1986):

$$\hat{F}_X(x|\{x_i,n\}) = \frac{1}{n}\sum_{i=1}^{n}\Phi\left(\frac{x-x_i}{\lambda_i h}\right)$$

where: $\Phi(u)$ is the cumulative distribution function of the standard normal distribution

h is the common smoothing factor e.g. the solution of the equation (Kijko, et al., 2001):

$$\sum_{i,j}\left\{2^{-0.5}\left[\frac{(x_i-x_j)^2}{2h^2}-1\right]exp\left[-\frac{(x_i-x_j)^2}{4h^2}\right]-2\left[\frac{(x_i-x_j)^2}{h^2}-1\right]exp\left[-\frac{(x_i-x_j)^2}{2h^2}\right]\right\} = 2n$$

λ_i are the local bandwidth factors e.g.: (Orlecka-Sikora & Lasocki, 2005)

$$\lambda_i = \left[\frac{\hat{f}^*(x_i|\{x_j,n\})}{g}\right]^{-0.5}$$

$$\hat{f}^*(x_i|\{x_j,n\}) = \frac{1}{\sqrt{2\pi}hn}\sum_{j=1}^{n} exp\left[-\frac{(x_i-x_j)^2}{2h^2}\right] \qquad g = \left[\prod_{i=1}^{n}\hat{f}^*(x_i|\{x_j,n\})\right]^{\frac{1}{n}}$$

The MATLAB toolbox with codes for equivalent dimension transformation can be downloaded from https://git.plgrid.pl/projects/EA/repos/sera-applications/browse

References:

Kijko, A., Lasocki S., & Graham G. (2001) Nonparametric seismic hazard analysis in mines. *Pure and Applied Geophysis*, 158, 1655-1676.

Lasocki, S. (2014) Transformation to equivalent dimensions – a new methodology to study earthquake clustering. *Geophysical Journal International*, 197 (2), 1224-1235.

Orlecka-Sikora, B. & Lasocki, S. (2005) "Nonparametric characterization of mining induced seismic sources." In: Proceedings Sixth International Symposium on Rockburst and Seismicity in Mines 9-11 March 2005, Australia, Potvin, Y., & Hudyma, M., Eds. (Australian Centre for Geomechanics, Nedlands 2005), pp. 555-560.

Silverman, B.W. (1986) "Density Estimation for Statistics and Data Analysis" (Chapman and Hall, London, 1986).

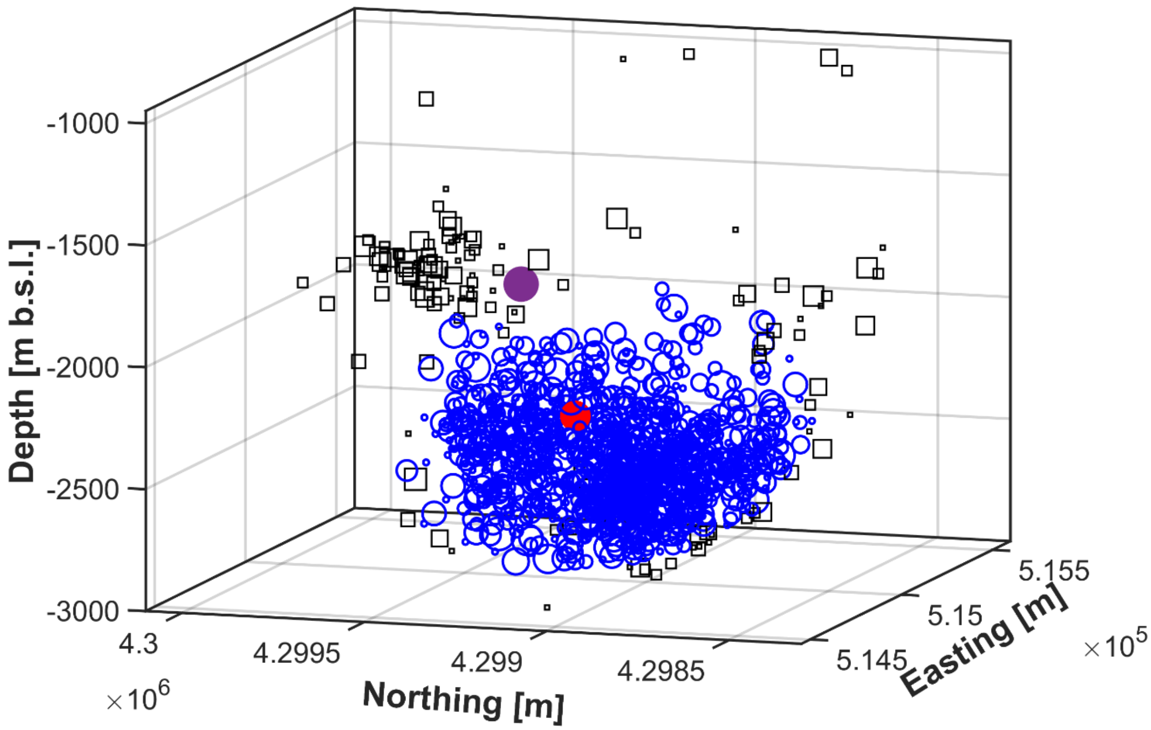

Figure S1. 3D view of spatial distribution of hypocenters of 1252 events from the seismic catalog from the NW region of The Geysers geothermal field. Blue circles indicate locations of the events from the cluster A, which have been analyzed in this paper. The other events from the initial dataset are marked by black squares. The size of markers is proportional to the magnitude of events. Big red dot marks the position of the open hole section of the Prati9 well and big violet dot marks the position of the open hole section of the Prati29 wells. The distances between the holes are: vertical – 386.8 m, horizontal – 479.5 m.

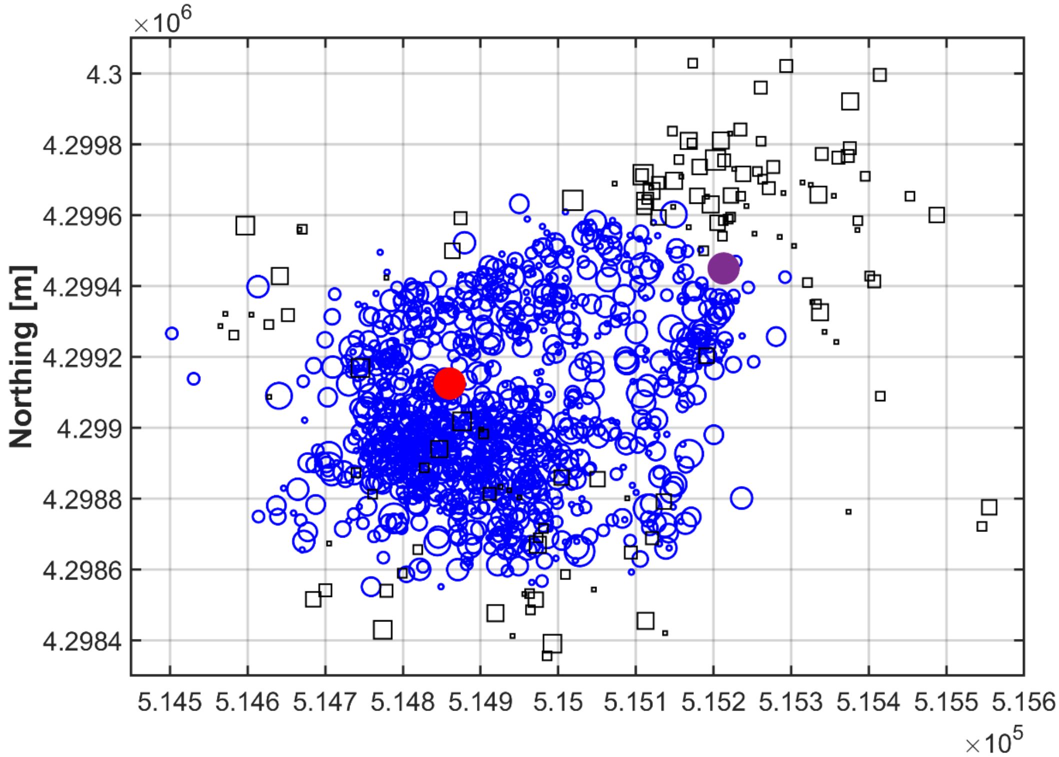

Figure S2. Horizontal projection of Figure S1.

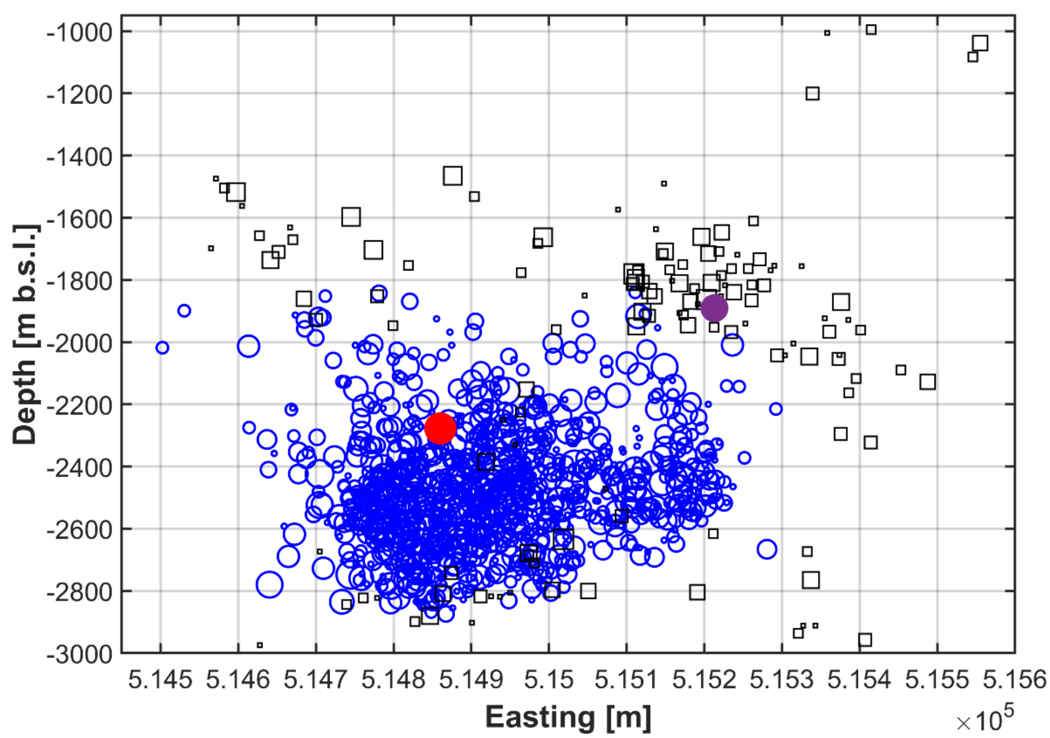

Figure S3. Vertical xz projection of Figure S2.

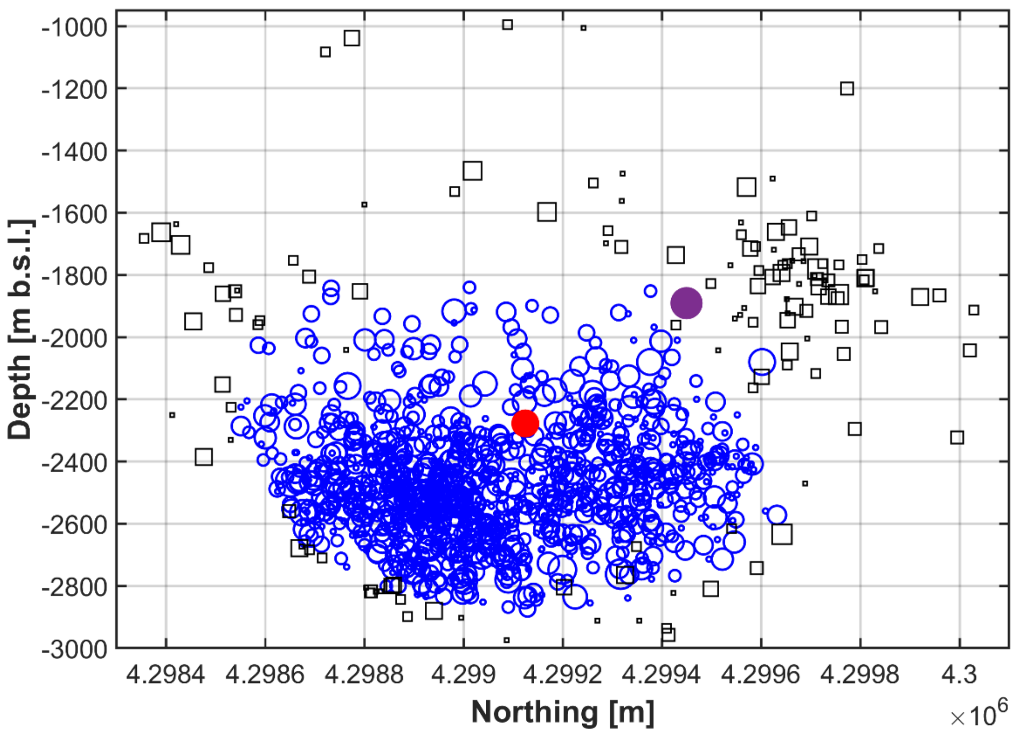

Figure S4. Vertical yz projection of Figure S2.

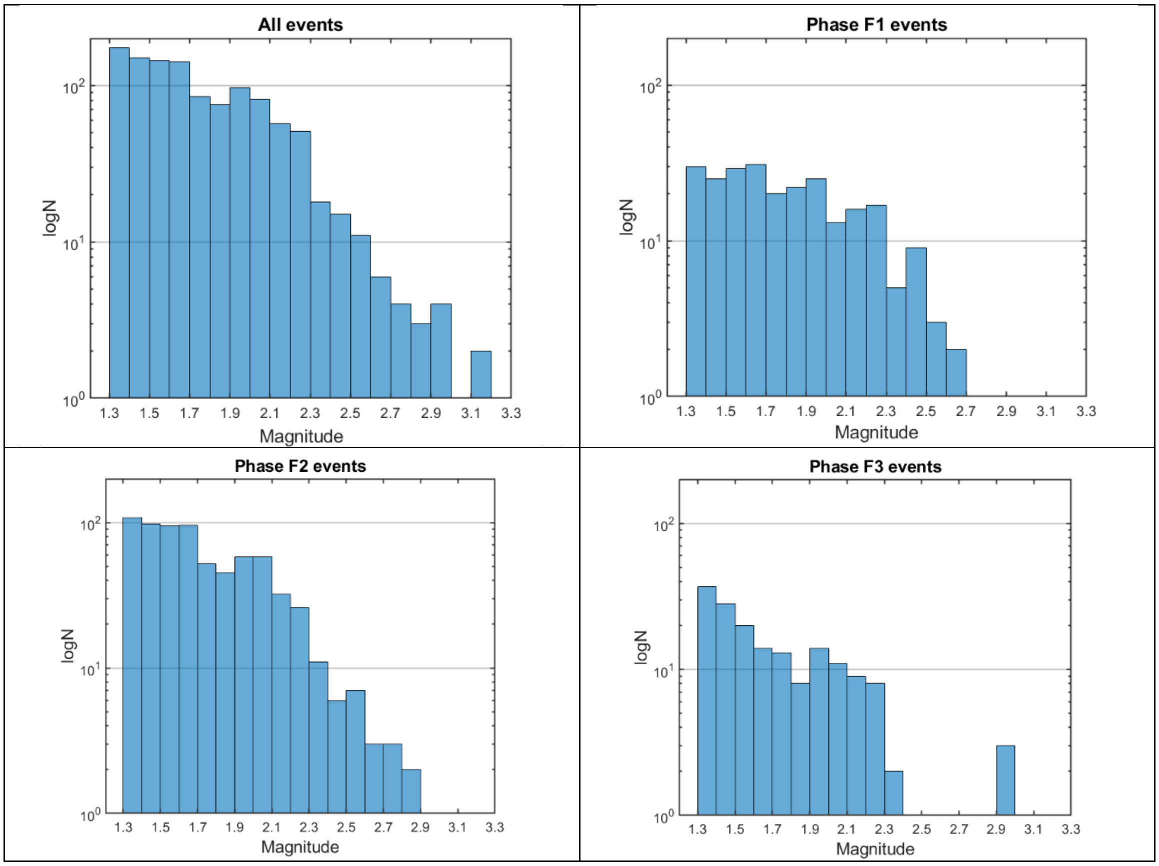

Figure S5. Magnitude-frequency histograms of studied events

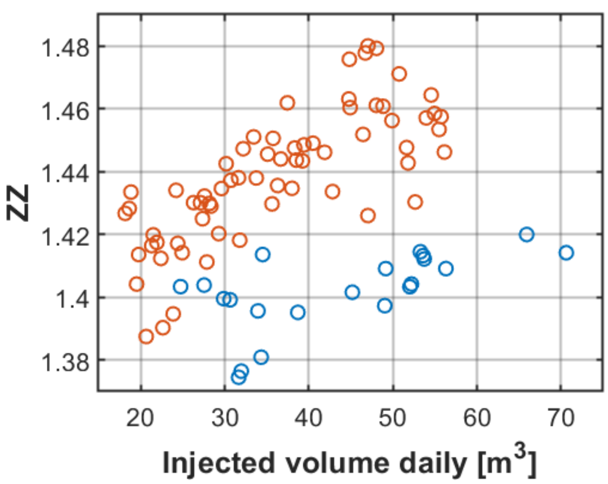

Figure S6. The degree of disordering of sources, ZZ vs. the average injection rate into Prati9 well, *IN*(9) scatterplots. Blue markers – the scatterplot for the injection phase F1. Brown markers – the scatterplot for the injection phase F2.

Table S1. Results of the correlation analysis between the average injection rate, *IN*, and the degree of disordering of seismic sources, *ZZ*, and its components, $\Delta_{\boldsymbol{r}}, \Delta_{\boldsymbol{M}}, \Delta_{\boldsymbol{\phi}}$ for the phase F1. The correlation have been evaluated for *ZZ*, $\Delta_{\boldsymbol{r}}, \Delta_{\boldsymbol{M}}, \Delta_{\boldsymbol{\phi}}$ delayed from 0 to 21 days with respect to *IN*.

Delay [days]	***ZZ***		Δ_r		Δ_M		Δ_ϕ	
	Corr. coef.	p-value	Corr. coef.	p-value	Corr. coef.	p-value	Corr. coef.	p-value
0	0.623	2.5E-03	0.694	4.9E-04	0.205	3.7E-01	-0.280	2.2E-01
1	0.621	2.7E-03	0.688	5.7E-04	0.210	3.6E-01	-0.275	2.3E-01
2	0.618	2.9E-03	0.682	6.6E-04	0.214	3.5E-01	-0.270	2.4E-01
3	0.614	3.0E-03	0.676	7.8E-04	0.219	3.4E-01	-0.265	2.5E-01
4	0.611	3.3E-03	0.669	9.1E-04	0.223	3.3E-01	-0.260	2.6E-01
5	0.607	3.5E-03	0.662	1.1E-03	0.227	3.2E-01	-0.255	2.6E-01
6	0.603	3.8E-03	0.654	1.3E-03	0.231	3.1E-01	-0.248	2.8E-01
7	0.599	4.1E-03	0.648	1.5E-03	0.235	3.1E-01	-0.244	2.9E-01
8	0.594	4.5E-03	0.641	1.7E-03	0.239	3.0E-01	-0.240	2.9E-01
9	0.590	4.9E-03	0.634	2.0E-03	0.243	2.9E-01	-0.236	3.0E-01
10	0.586	5.3E-03	0.627	2.3E-03	0.247	2.8E-01	-0.233	3.1E-01
11	0.581	5.7E-03	0.621	2.7E-03	0.250	2.7E-01	-0.229	3.2E-01
12	0.577	6.2E-03	0.614	3.1E-03	0.254	2.7E-01	-0.226	3.2E-01
13	0.572	6.7E-03	0.607	3.5E-03	0.257	2.6E-01	-0.223	3.3E-01
14	0.568	7.2E-03	0.602	3.9E-03	0.263	2.5E-01	-0.223	3.3E-01
15	0.563	7.8E-03	0.595	4.4E-03	0.266	2.4E-01	-0.220	3.4E-01
16	0.559	8.4E-03	0.588	5.0E-03	0.270	2.4E-01	-0.216	3.5E-01
17	0.554	9.1E-03	0.581	5.7E-03	0.274	2.3E-01	-0.213	3.5E-01
18	0.550	9.8E-03	0.574	6.5E-03	0.279	2.2E-01	-0.209	3.6E-01
19	0.545	1.1E-02	0.567	7.4E-03	0.283	2.1E-01	-0.206	3.7E-01
20	0.542	1.1E-02	0.560	8.2E-03	0.288	2.1E-01	-0.201	3.8E-01
21	0.538	1.2E-02	0.553	9.3E-03	0.292	2.0E-01	-0.198	3.9E-01

Table S2. Results of the correlation analysis between the average injection rate into Prati9 well, *IN*(9), and the degree of disordering of seismic sources, *ZZ*, and its components, $\Delta_r, \Delta_M, \Delta_\phi$ for the phase F2. The correlation have been evaluated for *ZZ*, $\Delta_r, \Delta_M, \Delta_\phi$ delayed from 0 to 21 days with respect to *IN*(9). The results based on Spearman rank correlation are in italics.

Delay [days]	***ZZ***		Δ_r		Δ_M		Δ_ϕ	
	Corr. coef.	p-value	Corr. coef.	p-value	Corr. coef.	p-value	Corr. coef.	p-value
0	0.756	2.2E-13	0.687	1.9E-10	0.408	6.7E-04	*0.493*	*3.4E-05*
1	0.759	1.5E-13	0.693	1.1E-10	0.409	6.6E-04	*0.488*	*4.1E-05*
2	0.761	1.2E-13	0.698	7.6E-11	0.409	6.5E-04	*0.482*	*5.1E-05*
3	0.762	1.1E-13	0.701	5.8E-11	0.407	6.9E-04	*0.481*	*5.4E-05*
4	0.762	1.1E-13	0.703	4.5E-11	0.407	7.1E-04	*0.481*	*5.3E-05*
5	0.764	9.0E-14	0.707	3.1E-11	0.407	7.0E-04	*0.478*	*6.1E-05*
6	0.765	7.4E-14	0.711	2.1E-11	0.407	6.8E-04	*0.475*	*6.9E-05*
7	0.767	6.0E-14	0.715	1.5E-11	0.408	6.7E-04	*0.472*	*7.6E-05*
8	0.768	5.0E-14	0.719	1.0E-11	0.408	6.7E-04	*0.467*	*9.3E-05*
9	0.770	4.2E-14	0.723	7.0E-12	0.408	6.8E-04	*0.456*	*1.4E-04*
10	0.771	3.6E-14	0.727	4.9E-12	0.407	6.8E-04	*0.454*	*1.5E-04*
11	0.772	3.1E-14	0.730	3.6E-12	0.408	6.8E-04	*0.447*	*1.9E-04*
12	0.773	2.8E-14	0.733	2.7E-12	0.409	6.5E-04	*0.441*	*2.5E-04*
13	0.774	2.5E-14	0.736	1.9E-12	0.409	6.5E-04	*0.444*	*2.2E-04*
14	0.775	2.2E-14	0.740	1.2E-12	0.407	6.9E-04	*0.440*	*2.6E-04*
15	0.776	2.0E-14	0.743	8.7E-13	0.407	6.9E-04	*0.435*	*3.0E-04*
16	0.777	1.8E-14	0.747	6.1E-13	0.407	7.0E-04	*0.430*	*3.6E-04*
17	0.777	1.6E-14	0.750	4.4E-13	0.407	7.0E-04	*0.427*	*3.9E-04*
18	0.778	1.5E-14	0.753	3.1E-13	0.407	7.0E-04	*0.422*	*4.7E-04*
19	0.778	1.5E-14	0.755	2.5E-13	0.406	7.2E-04	*0.417*	*5.5E-04*
20	0.778	1.4E-14	0.758	1.8E-13	0.406	7.2E-04	*0.410*	*6.9E-04*
21	0.778	1.4E-14	0.760	1.4E-13	0.407	6.8E-04	*0.406*	*8.0E-04*

Table S3. Results of the correlation analysis between the average of total injection rate into Prati9 and Prati29 wells, *IN*(both), and the degree of disordering of seismic sources, *ZZ*, and its components, $\Delta_r, \Delta_M, \Delta_\phi$ for the phase F2. The correlation have been evaluated for *ZZ*, $\Delta_r, \Delta_M, \Delta_\phi$ delayed from 0 to 21 days with respect to *IN*(both). The results based on Spearman rank correlation are in italics.

Delay [days]	***ZZ***		Δ_r		Δ_M		Δ_ϕ	
	Corr. coef.	p-value	Corr. coef.	p-value	Corr. coef.	p-value	Corr. coef.	p-value
0	0.722	7.7E-12	0.663	1.3E-09	0.452	1.4E-04	*0.472*	*7.6E-05*
1	0.723	6.9E-12	0.667	9.9E-10	0.453	1.4E-04	*0.466*	*9.7E-05*
2	0.723	6.8E-12	0.668	8.6E-10	0.453	1.3E-04	*0.472*	*7.8E-05*
3	0.723	7.0E-12	0.670	7.8E-10	0.451	1.4E-04	*0.477*	*6.3E-05*
4	0.721	8.4E-12	0.669	8.0E-10	0.450	1.5E-04	*0.476*	*6.6E-05*
5	0.721	8.6E-12	0.671	7.1E-10	0.450	1.5E-04	*0.470*	*8.4E-05*
6	0.721	8.9E-12	0.672	6.5E-10	0.451	1.5E-04	*0.462*	*1.1E-04*
7	0.720	9.1E-12	0.673	5.9E-10	0.451	1.5E-04	*0.465*	*1.0E-04*
8	0.720	9.3E-12	0.675	5.3E-10	0.450	1.5E-04	*0.466*	*9.8E-05*
9	0.720	9.4E-12	0.676	4.7E-10	0.449	1.5E-04	*0.467*	*9.4E-05*
10	0.720	9.6E-12	0.677	4.2E-10	0.448	1.6E-04	*0.474*	*7.2E-05*
11	0.721	9.1E-12	0.679	3.7E-10	0.448	1.6E-04	*0.475*	*6.8E-05*
12	0.720	9.7E-12	0.679	3.6E-10	0.448	1.6E-04	*0.476*	*6.5E-05*
13	0.719	1.0E-11	0.681	3.2E-10	0.447	1.7E-04	*0.479*	*5.7E-05*
14	0.720	9.9E-12	0.684	2.5E-10	0.445	1.8E-04	*0.476*	*6.5E-05*
15	0.719	1.0E-11	0.685	2.2E-10	0.444	1.9E-04	*0.471*	*7.9E-05*
16	0.719	1.0E-11	0.687	1.9E-10	0.443	1.9E-04	*0.465*	*1.0E-04*
17	0.719	1.0E-11	0.688	1.7E-10	0.442	2.0E-04	*0.460*	*1.2E-04*
18	0.719	1.1E-11	0.690	1.5E-10	0.442	2.1E-04	*0.460*	*1.2E-04*
19	0.718	1.2E-11	0.691	1.4E-10	0.439	2.2E-04	*0.457*	*1.3E-04*
20	0.718	1.2E-11	0.692	1.2E-10	0.439	2.3E-04	*0.458*	*1.3E-04*
21	0.717	1.3E-11	0.693	1.2E-10	0.440	2.2E-04	*0.462*	*1.1E-04*

Table S4. Results of the correlation analysis between the average of injection rate, *IN*, and the degree of disordering of seismic sources, *ZZ*, and its components, $\Delta_r, \Delta_M, \Delta_\phi$ for the phase F3. The correlation have been evaluated for *ZZ*, $\Delta_r, \Delta_M, \Delta_\phi$ delayed from 0 to 21 days with respect to *IN*.

Delay [days]	***ZZ***		Δ_r		Δ_M		Δ_ϕ	
	Corr. coef.	p-value	Corr. coef.	p-value	Corr. coef.	p-value	Corr. coef.	p-value
0	-0.603	2.9E-02	-0.199	5.1E-01	-0.321	2.8E-01	-0.195	5.2E-01
1	-0.587	3.5E-02	-0.176	5.6E-01	-0.338	2.6E-01	-0.183	5.5E-01
2	-0.571	4.2E-02	-0.154	6.2E-01	-0.354	2.3E-01	-0.171	5.8E-01
3	-0.554	4.9E-02	-0.131	6.7E-01	-0.371	2.1E-01	-0.159	6.0E-01
4	-0.538	5.8E-02	-0.108	7.3E-01	-0.387	1.9E-01	-0.147	6.3E-01
5	-0.521	6.8E-02	-0.085	7.8E-01	-0.403	1.7E-01	-0.135	6.6E-01
6	-0.505	7.8E-02	-0.063	8.4E-01	-0.420	1.5E-01	-0.123	6.9E-01
7	-0.485	9.3E-02	-0.035	9.1E-01	-0.438	1.3E-01	-0.111	7.2E-01
8	-0.469	1.1E-01	-0.013	9.7E-01	-0.454	1.2E-01	-0.098	7.5E-01
9	-0.452	1.2E-01	0.009	9.8E-01	-0.471	1.0E-01	-0.085	7.8E-01
10	-0.436	1.4E-01	0.031	9.2E-01	-0.488	9.1E-02	-0.072	8.2E-01
11	-0.419	1.5E-01	0.052	8.7E-01	-0.502	8.1E-02	-0.060	8.4E-01
12	-0.402	1.7E-01	0.074	8.1E-01	-0.519	6.9E-02	-0.047	8.8E-01
13	-0.386	1.9E-01	0.096	7.6E-01	-0.535	5.9E-02	-0.033	9.2E-01
14	-0.369	2.1E-01	0.117	7.0E-01	-0.552	5.1E-02	-0.019	9.5E-01
15	-0.352	2.4E-01	0.139	6.5E-01	-0.567	4.3E-02	-0.006	9.9E-01
16	-0.335	2.6E-01	0.161	6.0E-01	-0.582	3.7E-02	0.007	9.8E-01
17	-0.317	2.9E-01	0.182	5.5E-01	-0.597	3.1E-02	0.020	9.5E-01
18	-0.299	3.2E-01	0.204	5.0E-01	-0.610	2.7E-02	0.032	9.2E-01
19	-0.281	3.5E-01	0.225	4.6E-01	-0.622	2.3E-02	0.043	8.9E-01
20	-0.264	3.8E-01	0.247	4.2E-01	-0.640	1.9E-02	0.058	8.5E-01
21	-0.245	4.2E-01	0.268	3.8E-01	-0.651	1.6E-02	0.069	8.2E-01

Text S2. Comparison of the results of correlation analysis for different representations of closeness of hypocenters.

One of the three conditions which we expect to play a role in linking fractures and building for-reaching pathways for fluid migration is closeness of hypocenters. This condition is parameterized by the average distance between hypocenters in the space of hypocenter coordinates transformed to equivalent dimension, Δ_r. The transformation to equivalent dimensions was necessary to make comparable all eight used parameters of seismic events: three hypocentral coordinates, three independent angles determining orientations of the T and P axes of the double-couple focal mechanisms, and two angular coordinates of hypocenters in the spherical system beginning at the open hole of injection well. The comparability enabled, in turn, estimation of the degree of disordering of seismic sources, *ZZ*.

Δ_r significantly correlated with the injection rate, *IN*, in the injection phases F1 and F2. In phase F1 Δ_r was the only one component of *ZZ* whose correlation with *IN* was significant. It was then possible to apply in this phase another representations of closeness of hypocenters and compare their correlation results with the ones obtained for Δ_r. The metrics of distances between hypocenters in original Cartesian system is Euclidean. Making use of this fact we tried correlation dimension of distances between hypocenters, D_2, and summarized squared distances in the original (x,y,z) space, *d2*, as alternatives to Δ_r .

The correlation dimension estimate, D_2 was obtained using the integral correlation method (Grassberger & Procaccia, 1983; Lasocki & De Luca, 1998). D_2 is the slope of the straight line, which relates the number of pairs of sources whose mutual distances are smaller than a certain value of ε, with ε, in the double logarithmic scale.

The summarized squared distances in the original (x,y,z) space, *d2* was $\sum_{\substack{i,k \\ i\neq k}} (\boldsymbol{x_i} - \boldsymbol{x_k})^2$ where $\boldsymbol{x_\bullet}$ is the vector of hypocenter location in the original Cartesian system of coordinates.

Unlike Δ_r, D_2 did not correlated with *IN* at the prescribed significance level α=0.05. The Pearson correlation coefficient was 0.26, p=0.26. On the contrary *d2* was highly correlated with *IN*. The Pearson correlation coefficient was 0.87, $p=4\times10^{-7}$. We also analyzed correlation between *d2* and *IN* in phase F2, in which Δ_r significantly correlated with *IN* (corr. coeff. = 0.69, $p = 2\cdot10^{-10}$, see Main text Table 2). The Pearson correlation coefficient between *d2* and *IN* was 0.63, $p = 2\times10^{-8}$.

The correlation results with *d2*, same as those with Δ_r, validate positively the results with Δ_r because *d2* is the most basic measure of the total distance between hypocenters. The reason why the correlation between D_2 and *IN* was not ascertained were probably problems with accurate estimation of the correlation dimension of distance between hypocenters, D_2. In many data widows we could not distinguish correctly the linear part because the saturation and depopulation regions nearly overlapped. In the below graphs we present the *IN* vs. correlation dimension scatterplot and two plots of the correlation integral vs. threshold distance, which exemplify the difficulties with correct estimation of the correlation dimension.

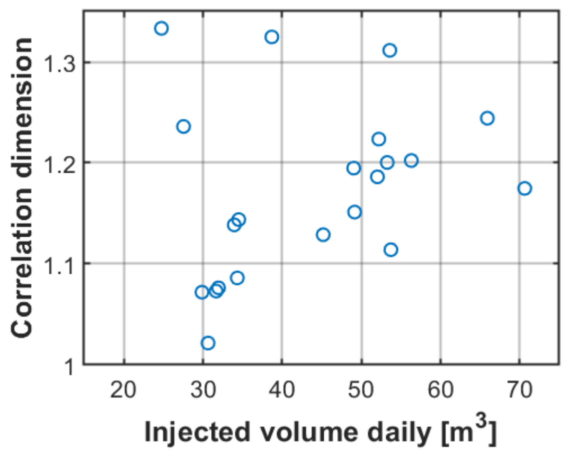

Figure Text S2-1. Scatter plot of correlation dimension of the distance between hypocenters, D_2 vs. injected volume into Prati9 well in phase F1, *IN*(9) .

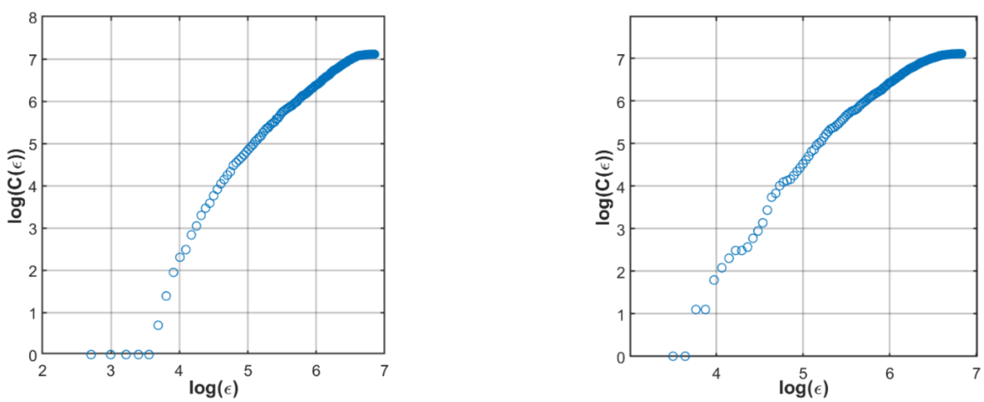

Figure Text S2-2. Two examples of the empirical relation between the correlation integral of the distance between hypocenters, $C(\varepsilon)$ and the threshold distance ε.

References:

Grassberger, P. & Procaccia, I. (1983) Measuring of strangeness of strange attractors. *Physica D*, 9, 189–208, https://doi.org/10.1016/0167-2789(83)90298-1.

Lasocki, S. & De Luca, L. (1998) Monte Carlo studies of relations between fractal dimensions in monofractal data sets. *Pure and Applied Geophysics*, 152, 213–220

Text S3. Discussion of the results of correlation analysis for phase F3 of injection.

In phase F3, in which the overall level of the injection rate, *IN*, was the lowest among injection phases, the correlation between *IN*, and the degree of disordering of sources, *ZZ*, was significant, negative. This correlation was achieved only jointly by the three components of *ZZ*: $\Delta_r, \Delta_M, \Delta_\phi$ because neither of the them significantly correlated with *IN* (Main text, Table 2). The negative correlation coefficient in F3 increased when *ZZ* was delayed with respect to *IN*, and for four and more days lag it became statistically not significant (Supporting Information Table S4).

The change of sign of the *IN* – *ZZ* correlation in F3 may be explained by the role of injection rate changes on the weakening/strengthening of rock. According to rock sample studies of Fjaer and Ruisten (2002) in rock weakening conditions there are many equivalent orientations of the failure plane, and the fracture orientation is determined by local weaknesses of the rock. In conditions of rock strengthening only two orientations for the potential failure plane fulfil the Coulomb failure criterion. Thence rock weakening conditions result in poorly ordered seismic fractures, and in rock strengthening conditions the fractures are better ordered. Orlecka-Sikora and Cielesta (2019) found two mutually reversed reactions of the stress field to injection rate changes in The Geysers, with the reversal point at some 50-70·10^2 m^3/day. At injection rates above this interval, increasing the injection rate enhanced rock weakening, and a decrease in the injection rate led to rock strengthening. Below this interval, the effect of injection rate variation was the opposite.

The injection rates in F1 and F2 were mostly above the aforementioned reversal point. To the contrary, the injection rates in F3 were well below this point. In the first two phases, weakening of the rock with increasing injection rate could favor the formation of randomly oriented fractures, which was expressed by the increase in the degree of disordering, *ZZ*. In F3 increasing the injection rate could lead to rock strengthening, which promoted the formation of fractures oriented in the optimal direction. As a consequence, the fractures were better ordered, which reduced *ZZ*.

We acknowledge, however, that since the data series in F3 was composed of only 13 points, the obtained *IN* – *ZZ* correlation ($p \approx 0.03$) might be spurious.

References:

Fjaer, E., & Ruistuen, H. (2002) Impact of the intermediate principal stress on the strength of heterogeneous rock, *Journal of Geophysical Research, Solid Earth*, 107, B2, 2032, doi: 10.1029/2001JB000277.

Orlecka-Sikora, B. & Cielesta, S. (2019) Evidence that the injection-induced earthquakes rupture subcritically. *Scientific Reports* (revised, under review)